Modelling of Capacitive MEMS Structures to Assess Reliability due to Charge Injection Processes

William D. Greason, Fellow, IEEE

Abstract - A parallel plate model is developed to analyze the effect of charge injection in capacitive microelectromechanical systems (MEMS). The electric fields and potential drops in the air gap and dielectric layer of the structure are calculated as a function of device geometry, switch state, operating voltage and trapped charge densities. Charge injection due to electrostatic discharge (ESD) events and triboelectrification is considered. The model is used to determine the conditions for the stiction phenomenon, dielectric and air gap breakdown.

Index Terms - charge injection, MEMS, model, reliability

I. INTRODUCTION

An analysis of the effect of electrostatic discharge (ESD) in capacitive microelectromechanical devices (MEMS) has been previously presented [1,2]. The following summary is included to serve as an introduction to the further work on the subject presented in this paper.

The basic parallel plate model of a capacitive MEMS structure is shown in Figure 1. The upper electrode, to be displaced by the application of control voltage V_0 has a plate area A and is separated from the fixed reference plate by a distance d; the gap medium is assumed to be air with a permittivity ε_0 . Attached to the bottom electrode is a thin dielectric layer of thickness d_0 and dielectric constant k; this layer is necessary to prevent a short circuit during the collapse of the plates. Typical parameters for a switch are:

Operating voltage: 10 V
Plate area: 100 x 100 μm^2
Plate spacing: 1-3 μm
Dielectric layer thickness: 0.2 μm

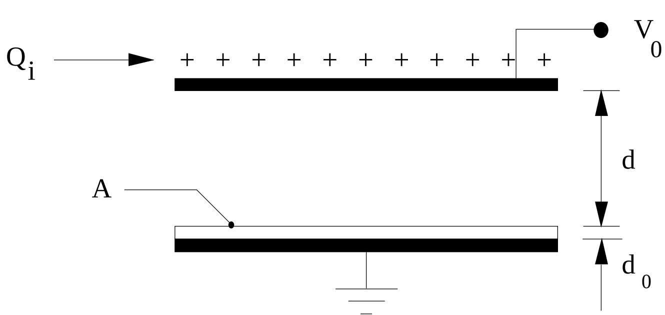

Fig. 1. Parallel plate model for capacitive MEMS

The modified Paschen's curve presented in Figure 2 applies for microgap assemblies. The slope of the modified curve in the region below approximately 4 μm is of the order of 7.5 x 10^7 $V.m^{-1}$.

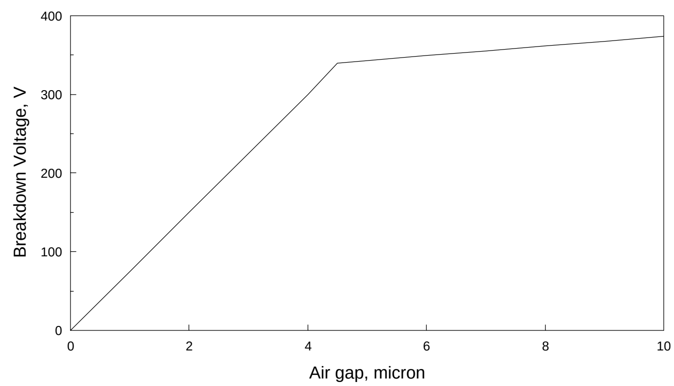

Fig. 2. Modified Paschen's curve

In the previous work, an analysis of the charge transfer in ESD events involving a charged source and a MEMS structure was presented. This included the human body model (HBM), charged device model (CDM) and the field charged device model (FCDM). In general, the charge transferred in an ESD event depends on the charge on the source body and the relative coupling of mutual electric flux between the source and the target. It was assumed that the charge transferred in the ESD event was imparted to the top electrode of the MEMS structure. ESD test methods that exist for semiconductor devices [3,4] are based on the direct injection of charge from a source to a pin of the device under test. The analysis included a charge injection model for the capacitive MEMS structure shown in Figure 1. It was concluded that in typical structures, breakdown of the air gap will result with the subsequent transfer of charge from the top electrode to the dielectric layer where it can become trapped.

II. OBJECTIVES

The objective of this work is to employ an electric field model of the MEMS structure to determine electric fields and potential drops in the air gap and dielectric layer of a MEMS structure as a function of switch geometry, switch state, control voltage and trapped charge. Results presented for a typical structure show the critical conditions to support air gap breakdown, dielectric breakdown and the onset of stiction.

III. ELECTRIC FIELD MODEL

The model shown in Figure 3 is used for the analysis. V_0 is the control voltage applied to the upper plate; the air gap separation is the variable x; the thickness of the dielectric layer with dielectric constant k is a. The surface charge density of the injected charge on the dielectric layer is $\sigma \quad C \cdot m^{-2}$. The electric fields in the air gap and dielectric are E_B and E_A respectively. The fields in the regions above and below the charge layer satisfy the boundary conditions [5]:

$$E_A a + E_B x = V_0 \qquad (1)$$

$$k\varepsilon_0 E_A - \varepsilon_0 E_B = \sigma \qquad (2)$$

The solutions for the electric fields in the air gap (E_B) and the dielectric (E_A) , and the potential drops across the air gap (V_B) and the dielectric layer (V_A) are:

$$E_A = \frac{V_0}{a}\frac{1}{1+kx/a} + \frac{\sigma}{k\varepsilon_0}\frac{1}{1+a/kx} \quad (3)$$

$$V_A = V_0\frac{1}{1+kx/a} + \frac{\sigma a}{k\varepsilon_0}\frac{1}{1+a/kx} \quad (4)$$

$$E_B = \frac{k\,V_0}{a}\frac{1}{1+kx/a} - \frac{\sigma}{\varepsilon_0}\frac{1}{1+kx/a} \quad (5)$$

$$V_B = V_0\frac{1}{1+a/kx} - \frac{\sigma a}{k\varepsilon_0}\frac{1}{1+a/kx} \quad (6)$$

In addition, for the modified Paschen's curve,

$$V_{BC} = k_1 x_C \quad (7)$$

where V_{BC} is the air gap voltage for breakdown and

k_1 = slope of modified Paschen's curve, 7.5×10^7 V.m^{-1}
x_C = critical air gap spacing for breakdown

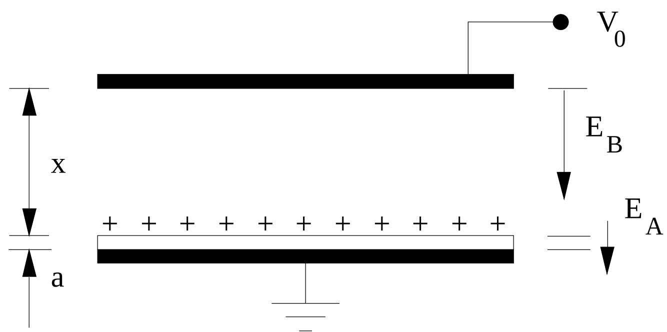

Fig. 3. Electric field model for capacitive MEMS structure

An analyses will be presented for the electric fields and voltage drops in the air gap and dielectric layer associated with a MEMS parallel plate structure. The possible modes of analysis include:

Normal operating mode: $V = V_0$, $\sigma = 0$; Charged dielectric only: $V = 0$, $\sigma = \sigma_0$; Normal operating mode with charged dielectric: $V = V_0$, $\sigma = \sigma_0$. The limiting cases include: plates open: x » a; plates closed: x « a.

From a review of equations (3) to (6), a/kx is chosen as the variable which defines the state of the plates. For a/kx « 1, the plates are open; for a/kx = 1; the plates are closing, for a/kx »1, the plates are closed. Graphs for the contribution to the voltage drop across the air gap due to the control voltage and the trapped charge in the dielectric are presented in Figures 4 and 5 respectively; graphs for the contribution to the electric field in the dielectric layer due to the control voltage and the trapped charge in the dielectric are presented in Figures 6 and 7 respectively.

The following observations are made. The equation for the air gap voltage V_B consists of two terms; one term due to the control voltage V_0 and one term due to the trapped charge σ. The magnitude of both terms decrease as the gap separation x is decreased. At any separation, a positive σ reduces the net V_B; a negative σ increase the net V_B. The equation for the electric field in the dielectric E_A also consists of two terms; one term is due to V_0 and one term is due to σ. As the gap is decreased, the magnitude of the contribution to E_A due to V_0 increases; the contribution due to σ decreases. At any separation and a positive V_0, the contributions are additive for a positive σ and subtractive for a negative σ.

The following assumptions for the model will be made.

(1) A uniform field geometry
(2) Uniform charge distribution on the dielectric layer
(3) Any space charge effects due to discharge are negligible

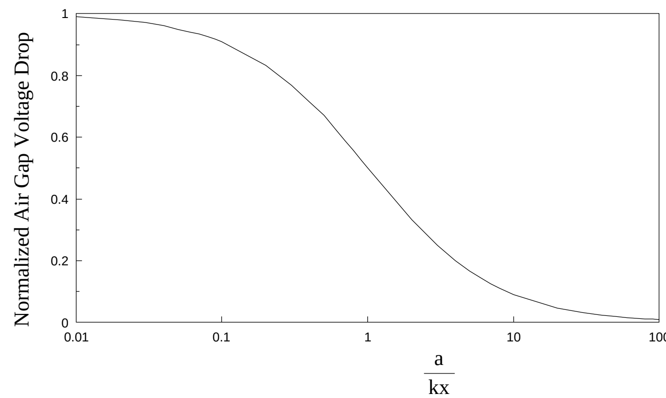

Fig. 4. Air gap voltage drop due to control voltage normalized to V_0 vs gap factor a/kx

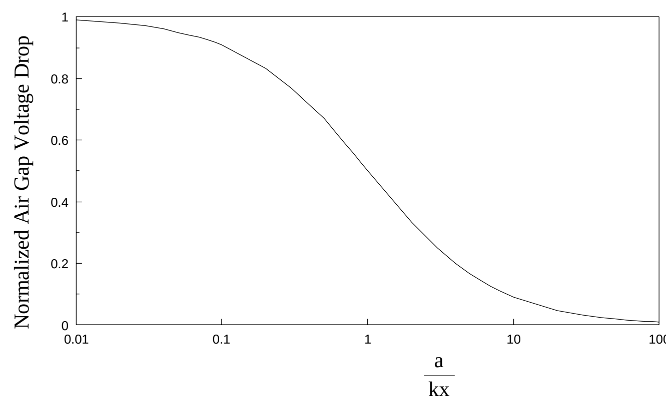

Fig. 5. Air gap voltage drop due to surface charge density normalized to $(\sigma a)/(k\varepsilon_0)$ vs gap factor a/kx

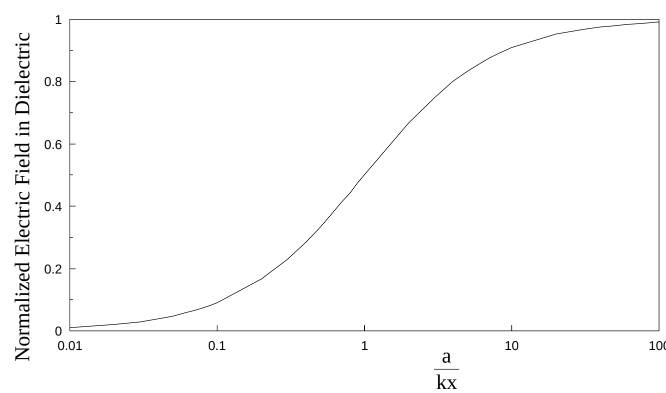

Fig. 6. Electric field in dielectric due to control voltage normalized to V_0/a vs gap factor a/kx

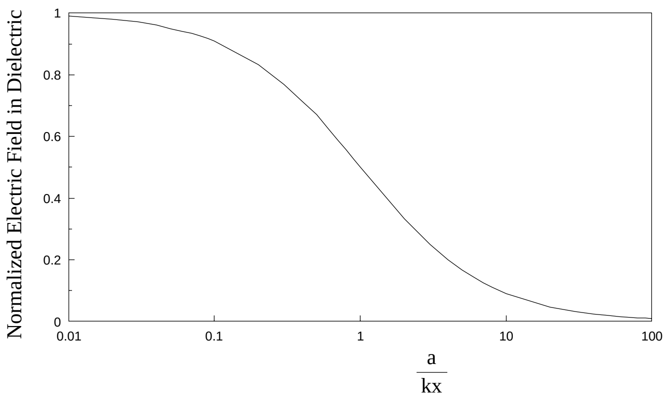

Fig. 7. Electric field in dielectric due to surface charge density normalized to $\sigma/(k\varepsilon_0)$ vs gap factor a/kx

IV. CHARGE INJECTION PROCESSES

A. ESD

Charge injection processes due to ESD have been analyzed in the previous work. Since triboelectrification is the charging mechanism for the source body, both polarities for the trapped charge σ are possible. The magnitude of σ depends on the charge on the source body and the relative coupling of electric flux between the source and target bodies.

B. Triboelectrification

Charge is injected into the dielectric layer as a result of contact and separation between the top electrode and the dielectric. The polarity of σ will depend on the materials employed as charging partners. In the absence of dissipation processes, the total charge will increase due to repeated contacts and separations.

The maximum surface charge density can be calculated using Gauss' law and the appropriate breakdown strength of air. Consider a thin dielectric layer of surface are A with surface charge density σ due to triboelectrification as shown in Figure 8. Then,

$$\oint D \cdot dA = Q$$

$$2\varepsilon_0 EA = \sigma A$$

$$\sigma = 2\varepsilon_0 E \qquad (8)$$

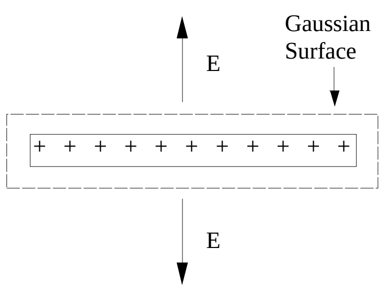

Fig. 8. Electric field for dielectric layer with surface charge density σ $C \cdot m^{-2}$.

Assuming that the electric flux associated with the surface charge is distributed equally between the two surfaces and using a value of 7.5 x 10^7 $V.m^{-1}$ for the breakdown strength of air for a parallel plate geometry with gaps less than 4 µm, the maximum surface charge density can be calculated.

$$\sigma_{max} = 0.66 \times 10^{-3}\ C.m^{-3}$$

If the flux associated with the surface charge is limited to one surface, the maximum surface charge density becomes:

$$\sigma_{max} = 1.33 \times 10^{-3}\ C.m^{-3}$$

C. Air Gap Breakdown

Charge is transferred across the air gap due to breakdown predicted by the modified Paschen's curve. The polarity of σ will be of the same polarity as the potential V_0 on the injecting electrode. For repeated opening and closing of the switch, an iterating procedure involving subsequent discharges is involved until the minimum gap for the design is reached or until the gap voltage V_B approaches zero. The calculation procedure for two cycles of this iterating procedure follows.

Cycle One

$\sigma = 0$

Solve for x_0 for breakdown, where:

$$V_B = k_1 x_0$$

Then:

$$x_0 = V_0/k_1 - a/k$$

σ_0 is transferred across the gap, where:

$$V_B = k_1 x_0$$

$$C = \varepsilon_0 A/x_0$$

$$Q = CV$$

$$\sigma_0 = Q/A = k_1 \varepsilon_0$$

Recalculate V_B using equation (6) with $\sigma = \sigma_0$.

The switch is opened; recalculate V_B using equation (6).

Cycle Two

Reduce x and solve for x_1 for breakdown.

$$x_1 = V_1/k_1 - a/k$$

where:

$$V_1 = [V_0 - (\sigma a)/(k\varepsilon_0)]$$

Prior to discharge, calculate V_B using equation (6).

σ is transferred across the gap.

Recalculate V_B using equation (6) with $\sigma = 2\ \sigma_0$.

The switch is opened; recalculate V_B using equation (6).

V. ANALYSIS

Various reliability issues will be analyzed and example calculations presented for the following typical test structure.

Area: 100 x 100 μm^2
Air gap: 3 μm
Dielectric thickness: 0.2 μm
Dielectric breakdown: 10^7 V.cm^{-1}
Dielectric constant: 5
Operating voltage: 10V

A. Air Gap Breakdown

The iterating procedure was repeated for three switch cycles. A plot of the air gap voltage as a function of air gap for the case where the switch is closed is shown in Figure 9. The air gap voltage as a function of switch cycles for the case where the switch is open in presented in Figure 10. As a result of repeated discharges, the net V_B approaches zero. This can be interpreted as a possible condition to support the onset of stiction.

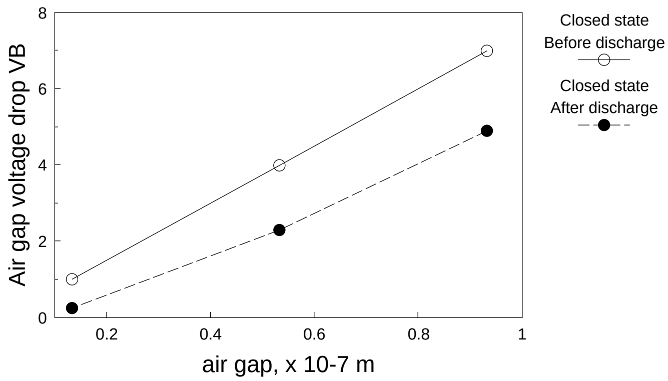

Fig. 9. Air gap voltage V_B with switch in closed state versus air gap x

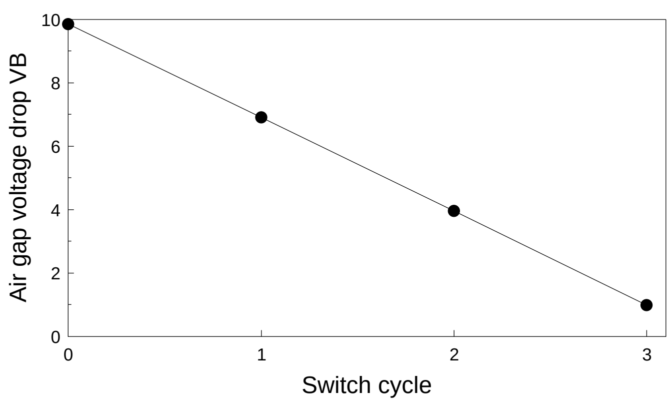

Fig. 10. Air gap voltage V_B with switch in open state versus switch cycle

B. Stiction

The general expression for the air gap voltage drop is:

$$V_B = V_0 \frac{1}{1+a/kx} - \frac{\sigma a}{k\varepsilon_0} \frac{1}{1+a/kx} \quad (9)$$

The following interpretation can also be made concerning the condition where the net air gap voltage drop V_B approaches zero due to equal but opposite voltage drop contributions due to V_0 and σ; this condition applies for the case where both V_0 and σ are positive . If the switch is closed and V_0 is removed, the force due to σ will result in the switch remaining closed. If V_0 is now applied, the net V_B is zero and the switch will open. If the switch is open and V_0 is removed, the force due to σ will cause the switch to close. There appears to be an inversion between switch state and control voltage due to the trapped charge σ.

When the control voltage V_0 is positive and the trapped charge σ is negative, the following interpretation applies when the voltage drops due to V_0 and σ become equal in magnitude. For both switch states, the electrostatic force due to the net V_B will cause the switch to close or remain closed; this in then the condition for stiction.

Both terms in this expression have a maximum when the switch is open and decrease as the switch is closed. Equating the two terms will yield the surface charge density which gives the same voltage drop as due to the control voltage V_0. This can be interpreted as the condition to initiate false closure of the plates or the onset of stiction.

$$V_0 \frac{1}{1+a/kx} = \frac{\sigma a}{k\varepsilon_0} \frac{1}{1+a/kx}$$

$$\sigma = \frac{V_0 k \varepsilon_0}{a} \quad (10)$$

For the test structure, this gives σ = 2.2x10^{-3} C · m^{-2}.

C. Dielectric Breakdown

In the absence of a control voltage, the maximum electric field E_A in the dielectric is realized when the switch is open. Assuming kx >> a,

$$E_A = \frac{\sigma}{k\varepsilon_0} \quad (11)$$

It is possible to solve for the surface charge density for dielectric breakdown.

$$\sigma = k\varepsilon_0 E_{BD}$$

For the test example, σ = 44.25 x 10^{-3} C · m^{-2}.

VI. SUMMARY

An electric field model has been presented for use in the analysis of the effect of charge injection in MEMS structures. Air gap voltage drops and electric fields in the dielectric layer can be calculated as a function of switch geometry, switch state, control voltage and trapped charge. Conditions for stiction and dielectric breakdown are developed.

ACKNOWLEDGMENT

The author acknowledges with thanks the financial support of the National Sciences and Engineering Research Council of Canada.

REFERENCES

[1] W.D. Greason, "Analysis of charge injection processes including ESD in MEMS", Journal of Electrostatics, Vol. 66, Nos. 11-12, November 2008, pp. 602-608.

[2] W.D. Greason, "Effect of charge injection due to ESD on the operation of MEMS", Conference Record, IEEE Industry Applications 42nd Annual Meeting, New Orleans, LA, USA, September 23-27, 2007, pp. 2188-2193. Revised paper accepted for publication in IEEE Transactions on Industry Applications, 2008.

[3] ANSI/ESD STM 5.1-2007, ESD Association Standard Test Method for Electrostatic Discharge Sensitivity Testing - Human Body Model (HBM) Component Level, Electrostatic Discharge Association, Rome, NY, 2007.

[4] ANSI/ESD STM 5.3.1-1999, ESD Association Standard Test Method for Electrostatic Discharge Sensitivity Testing - Charged Device Model (CDM) Component Level, Electrostatic Discharge Association, Rome, NY, 1999.

[5] J.M. Crowley, *Fundamentals of Applied Electrostatics.* Laplacian Press, Morgan Hill, CA, 1999.